King Saud University

Arabian Journal of Chemistry

ORIGINAL ARTICLE

Ecofriendly and sustainable *Sargassum* spp.-based system for the removal of highly used drugs during the COVID-19 pandemic

J. Luis López-Miranda [a], Gustavo A. Molina [a], Rodrigo Esparza [a], Marlen Alexis González-Reyna [a], Rodolfo Silva [b], Miriam Estévez [a],*

[a] *Centro de Física Aplicada y Tecnología Avanzada, Universidad Nacional Autónoma de México, Boulevard Juriquilla 3001, Querétaro 76230, Mexico*
[b] *Instituto de Ingeniería, Universidad Nacional Autónoma de México, Edificio 17, Ciudad Universitaria, Coyoacán, Mexico City 04510, Mexico*

Abstract Analgesic consumption increased significantly during the COVID-19 pandemic. A high concentration of this kind of drug is discarded in the urine, reaching the effluents of rivers, lakes, and seas. These medicines have brought serious problems for the flora and, especially, the ecosystems' fauna. This paper presents the results of removing diclofenac, ibuprofen, and paracetamol in an aqueous solution, using *Sargassum* spp. from the Caribbean coast. The study consisted of mixing each drug in an aqueous solution with functionalized *Sargassum spp* in a container under constant agitation. Therefore, this work represents an alternative to solve two of the biggest problems in recent years; first, the reduction of the overpopulation of sargassum through its use for the remediation of the environment. Second is the removal of drug waste used excessively during the COVID-19 pandemic. Liquid samples of the solution were taken at intervals of 10 min and analyzed by fluorescence to determine the concentration of the drug.

The sorption capacity for diclofenac, ibuprofen, and paracetamol was 2.46, 2.08, and 1.41 μg/g, corresponding to 98 %, 84 %, and 54 % of removal, respectively. The removal of the three drugs was notably favored by increasing the temperature to 30 and 40 °C, reaching efficiencies close to 100 %. Moreover, the system maintains its effectiveness at various pH values. In addition, the *Sar-*

* Corresponding author.
E-mail addresses: lopezfim@gmail.com (J. Luis López-Miranda), gustavomolina21@gmail.com (G.A. Molina), resparza@fata.unam.mx (R. Esparza), marlengonzalez@fata.unam.mx (M. Alexis González-Reyna), bmiries@fata.unam.mx (R. Silva), miries@fata.unam.mx (M. Estévez).

Production and hosting by Elsevier
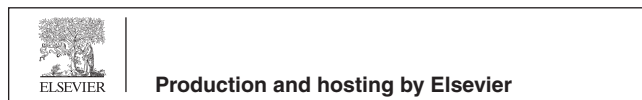
gassum used can be reused for up to three cycles without reducing its removal capacity. The wide diversity of organic compounds favors the biosorption of drugs, removing them through various kinetic mechanisms. On the other hand, the *Sargassum* used in the drugs removal was analyzed by X-ray diffraction, FTIR spectroscopy, TGA analysis, and scanning electron microscopy before and after removal. The results showed an evident modification in the structure and morphology of the algae and demonstrated the presence of the biosorbed drugs. Therefore, this system is sustainable, simple, economical, environmentally friendly, highly efficient, and scalable at a domestic and industrial level that can be used for aquatic remediation environments.

1. Introduction

Water is vital to the continued existence of all known life forms on earth. It is a unique resource that cannot be substituted; nevertheless, it has been constantly contaminated by various organic and inorganic pollutants due to the improper treatment of industrial waste and disposal of domestic waste (Ademollo et al. 2021, Awoyemi et al. 2021, Zhang et al. 2021). Some contaminants are emerging and unregulated compounds with toxic or mutagenic activity; then, their presence in the environment is not desirable because of their effect on flora and fauna (Lapworth et al. 2012, Luo et al. 2014, Sui et al. 2015). Examples of compounds that have recently emerged as particularly relevant are surfactants, pharmaceuticals, personal care products, gasoline additives, fire retardants, antiseptics, industrial additives, and pesticides (Mahmoud et al. 2021). Of all the emerging contaminants, the ones that probably cause the most significant concern are medicines. Their study is among the priority lines of research of leading organizations dedicated to protecting the public and environmental health, such as the World Health Organization, the Environmental Protection Agency, and the European Commission (de Wilt et al. 2016, Cardoso-Vera et al. 2021). Some of the most used medications are analgesics and anti-inflammatories. The consumption of this kind of drugs increased significantly during the COVID-19 pandemic.Table 1..

In December 2019, the first cases of the disease caused by severed acute respiratory syndrome coronavirus 2 (SARS-CoV-2) appeared in Wuhan, China. In the first months of 2020, this disease in countries around the world had already affected over 200 people. Initially, the pandemic hit the United States, Spain, and Italy the most (Yunus et al. 2020). However, the pandemic effects were reflected not only in the economy and social relationships but also in the environment. The latter is widely commented on in the scientific literature, (pollution of wastewater with anti-inflammatory and antiviral drugs, personal protective equipment, etc.) (Rupani et al. 2020, Shakil et al. 2020, Usman et al. 2020, Yunus et al. 2020).

Today, a significant concern worldwide is defeating COVID-19 and avoiding more deaths and new infections. The generation of hospital waste and the consumption of certain drugs have increased exponentially since the pandemic generated by the virus SARS-CoV-2 (Kitajima et al. 2020). In the initial period of the pandemic, known anti-viral, anti-malarial and anti-inflammatory drugs were introduced into treatment. Non-steroidal anti-inflammatory drugs (NSAIDs) have also been widely used in the treatment of Covid-19, especially in patients treated at home. With over-the-counter availability, they are often used without medical supervision to treat the basic symptoms of COVID-19, and NSAIDs can be found in the sewage treatment plant along with domestic and hospital sewage (Barcelo 2020). After reaching the sewage plant, these drugs undergo a partial biological or chemical transformation, often into intermediates with a higher toxicity than the parent drug (Marchlewicz et al. 2017).

NSAIDs stand out due to the large amount consumed each year, their widespread occurrence, and the concerns about their bioactivity and toxicity in water. Their low price and wide availability make them the preferred drugs to be prescribed for common complaints such as pain and inflammation, in addition to self-medication, contributing to the high consumption of these pharmaceuticals (Parolini 2020). They are among the most commonly consumed medications either by prescription or overthe-counter (Osafo et al. 2017). Today, > 50 different NSAIDs are available on the global pharmaceutical market, and almost 35 million people use them daily (Fokunang et al. 2018). Among the most popular NSAIDs today, apart from acetylsalicylic acid, are ibuprofen, diclofenac, naproxen, ketoprofen, piroxicam, mefenamic acid, celecoxib or rofecoxib (Osafo et al. 2017).

Due to their hydrophilicity and stability, they tend to remain in the aqueous phase and are not eliminated in the treatment plants. So these and their metabolites are frequently detected in the water superficial at concentrations from several ng/L (for example, in seawater) to even mg/L in the case of effluents from the pharmaceutical industry (Zhang et al. 2020).The most frequently detected drugs were diclofenac, ibuprofen, naproxen, paracetamol, acetaminophen and ketoprofen (Omotola and Olatunji, 2020, Thalla and Vannarath, 2020, Jurado et al. 2021, (Madikizela and Ncube, 2021), Praveenkumarreddy et al. 2021, Reinstadler et al. 2021). High concentrations of NSAIDs in the environment are also observed on the European continent. For example, in the Besós river flowing through the urbanized areas of the metropolitan district of Barcelona (Spain), the following NSAIDs were detected, ketoprofen (42–133 ng/L), ibuprofen (73–126 ng/L), diclofenac (199–469 ng/L), mefenamic acid (8–13 ng/L), salicylic acid (54–109 ng/L), propyphenazone (14–85 ng/L) and phenazone (5–37 ng/L). The high concentration of diclofenac corresponded to the identified 4-hydroxy derivative metabolite. In addition, the appearance of the studied drugs in this region was also shown in the aquifer (Jurado et al. 2021).

Also on the South American continent, the occurrence of high concentrations of paracetamol and diclofenac and their high environmental risk have been observed. Paracetamol concentrations even above 500 µg/L were found in the sewage treatment plants in Juliaca (Peru) (Nieto-Juárez et al. 2021).

For example, ibuprofen (IBU) is a non-steroidal anti-inflammatory drug used for medical treatment in humans and animals. Since IBU is not entirely absorbed in the body, a portion of it is obviously defecated and entered the aqueous environment. Besides, IBU can be fed to the natural environment through pharmaceutical industry wastes. Its elimination efficiency has been reported to be up to 90 % in treatment plants; however, due to the large amounts introduced into the environment, a critical pseudo-persistence effect is present, having traumatic consequences in nature. Because of the chronic toxicity demonstrated, this drug may represent a real threat to organisms in contact with this substance, even at very low concentrations (Pomati et al. 2004, Santos et al. 2010). In fact, it can widely endanger human life and the health of the natural habitat (Costa et al. 2021). Paracetamol (PCT) (N-(4-hydroxyphenyl) acetamide), also known as acetaminophen, is one of the most widely used analgesics and antipyretics worldwide (Costa et al. 2021). Its high consumption implies a continuous discharge in aqueous environments through industrial and domestic wastewater that requires mitigation and remediation strategies. Due to its high stability, solubility, and hydrophilicity, it has been detected in surface waters, wastewater, and drinking water throughout the world

(Cleuvers 2004, Bonnefille et al. 2018). The use of microalgae for the biosorption of paracetamol has been reported (Escapa et al. 2017); the removal percentages were from 41 % to 69 %, depending on the initial concentration of the drug. Diclofenac sodium (DCF) is an analgesic drug generally prescribed to treat inflammatory disorders because of its non-steroidal anti-inflammatory potential. The DCF neutral form presents free acid groups (–COOH), whereas the anionic form presents deprotonated acid groups (–COO −). Chronic exposure to DCF generates hemodynamic changes and thyroid tumors in Humans. The removal of this drug by diosorption processes has been previously reported, reaching an efficiency between 70 and 80 % (Hifney et al. 2021). Furthermore, adverse effects have been observed on natural ecosystems, causing the death of several animal species (Alothman et al. 2020).

The removal of these types of drugs by means of treatment plants has been inefficient (Mir-Tutusaus et al. 2016). Therefore, several methods, including the use of fungi (Dalecka et al. 2021), membranes (Li et al. 2022), and hybrid materials (Nava-Andrade et al. 2021), have been investigated for these purposes. However, some of them require expensive and/or complex processes. Biosorbent materials are among the most promising approaches due to their low cost, high efficiency, and being environmentally friendly (Bimová et al. 2021, Huang et al. 2021, Neha et al. 2021). In this sense, it has been reported that *Sargassum* spp. has biosorbent properties with the ability to trap various substances, such as organic dyes (López-Miranda et al. 2020). *Sargassum* belongs to the brown algae family. There are several species of *Sargassum* with differences in their chemical composition and characteristics. In this study, the *Sargassum* spp. that reaches the Mexican Caribbean coast was used, which consists of two species: *S. natans* and *S. fluitans* (Vázquez-Delfín et al. 2021). This type of algae has recently been investigated due to the overpopulation that arrives at the Mexican coasts, bringing alterations in the ecosystem and economic problems (Chávez et al. 2020, Robledo et al. 2021). Therefore, various uses and applications have been given to it according to its compounds and properties (Miranda et al. 2021). Among its main compounds are alginates, a permeable compound attributed to the sorption capacity. In addition, this removal property can be increased by subjecting *Sargassum* spp. to a chemical treatment (López-Miranda et al. 2020). Therefore, in this work the use of *S. natans* and *S. fluitans* for the removal of drugs consumed during the COVID-19 pandemic (DFS, PCT, and IBU) is reported for the first time, being a simple, economical and highly efficient method. Even more, the concentration of the drug in solution is commonly carried out using high-performance liquid chromatography (HPLC) (Coimbra et al. 2018, Santaeufemia et al. 2018, Parus et al. 2020), which requires the use of special separation columns and different solvents. Here we propose the use of carbon dots to quantify the concentration by means of fluorescence intensity variations.

2. Experimental

2.1. Materials

Sargassum spp. referred it as *Sargassum* for the rest of the manuscript (59.3 % *S. fluitans*, 35.8 % *S. natans* I, 3.3 % benthic microphytes, and 1.4 % *S. natans* VIII (Vázquez-Delfín et al. 2021)) used in this work was collected in Puerto Morelos Quintana Roo (20°50′44.1″N, 86°52′35.5″W) in June 2021. Hydrogen peroxide (30 % w/w in H_2O) from Sigma Aldrich to treat *Sargassum*. The drugs paracetamol (acetaminophen, BioXtra, ≥99 %), diclofenac sodium (>98 %, TLC), and ibuprofen (>98 %, GC), all analytical grade, were purchased from Sigma-Aldrich. The pH was adjusted with NaOH (BioXtra, >98 %, pellets-anhydrous) from Sigma Aldrich. All reactants were used as received. All aqueous solutions were made with deionized water.

2.2. Chemical treatment of Sargassum.

The *Sargassum* was washed several times with deionized water to remove impurities, garbage, and sand. Subsequently, it underwent a treatment consisting of placing 500 g of *Sargassum* in a 20 % solution of hydrogen peroxide for 24 h. The *Sargassum* was then rewashed with deionized water and left to dry in the shade for a week. Finally, the *Sargassum* was stored under refrigeration for later use.

2.3. Synthesis of carbon dots (CDs)

Clean, and dry *Sargassum* was pulverized using a 1000 W domestic blender and passed through a 150-mesh sieve (106 μm). Then 1 g of the Sargassum powder was mixed with 50 mL of 50 % water/isopropanol using magnetic stirring at 60 °C for 30 min. Subsequently, the liquid phase was recovered by filtration using Whatman #41 filter paper. Following that, CDs have been synthesized by hydrothermal treatment using the Sargassum extract as a natural precursor. In the hydrothermal synthesis, the aqueous suspension was heated at 250 °C using a Teflon-lined autoclave for 12 h. After synthesis, the supernatant was collected and evaporated. Then, the dry solid was redissolved in deionized water and centrifuged at 5000 rpm for 10 min to remove larger particles. Pure CDs with blue fluorescence can finally be obtained through a 200 nm filter membrane. The product solution was lyophilized and stored until further use.
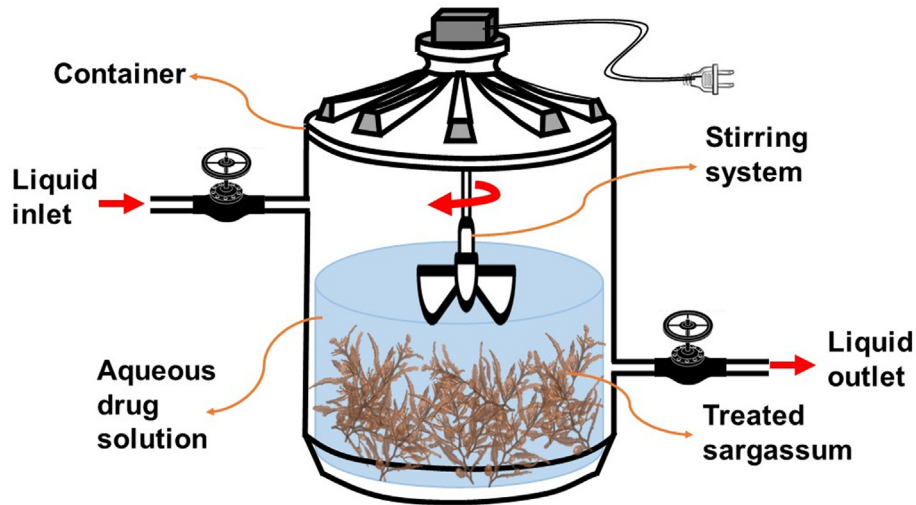
2.4. Drug removal

Drug removal was carried out using the system shown in scheme 1, which consists of a container with a constant agitation system. In the walls are the inlet and outlet pipes, which are connected to regulation valves. The removal process consisted of placing and mixing 3.0 g of *Sargassum* with 500 mL of PCT at 15 ppm inside the container. Then, 10 mL samples were taken at intervals of 10 min until completed 2 h. After this time, the *Sargassum* was removed and left to dry in the shade for later characterization. This process was repeated for IBU and DFS.

The *Sargassum* removal capacity was evaluated using the algae repeatedly. The same procedure was carried out for PCT, IBU, and DFS. The *Sargassum* used in the removal was recovered, washed with deionized water, and dried; later, this same *Sargassum* was used to carry out the removal of the drug. This process was repeated until completing the four cycles.

2.5. Drug quantification

Fluorescence spectrophotometry (from 400 to 700 nm) was obtained with a Varioskan Flash microplate reader (Thermo Fisher Scientific, Waltham, MA, United States) using 360 nm as excitation wavelength. DFS, IBU, and PCT concentrations from 0 to 15 ppm were mixed with 50 μg/mL of carbon dots (CDs) to perform the calibration curve. Then, the analysis was centered at 480 nm, where higher fluorescence intensity was found for each sample.

Scheme 1   System used for the drug removal using *Sargassum* as biosorbent material.

With the obtained data, the sorption capacity (amount of the selected drug per unit weight of *Sargassum* at time *t*) was estimated using the following expression:

$$q_e = \frac{V}{w}(C_i - C_t) \cdots \tag{1}$$

where C_i is the initial concentration of the selected drug, C_t the drug concentration (mg/L) at a given time *t*, *V* the volume of the solution (L), and *w* the weight of *Sargassum* used as biosorbent (g).

Using the data collected, the remotion efficiency, *R (%)*, was calculated using equation (2):

$$R(\%) = \frac{C_i - C_t}{C_i} \times 100\% \cdots \tag{2}$$

where C_i is the initial concentration of the selected drug, C_t the drug concentration (mg/L) at a given time *t*.

Moreover, the distribution coefficient (K_d) was calculating to observe the chemical affinity between the drug and the algae:

$$K_d = \frac{V}{w}\left(\frac{C_i - C_t}{C_t}\right) \cdots \tag{3}$$

where C_i is the initial concentration of the selected drug, C_t the drug concentration (mg/L) at a given time *t*, *V* the volume of the solution (L), and *w* is the mass use of *Sargassum* for biosorption (g).

2.6. Determination of kinetic parameters

The kinetic parameters were calculated to evaluate the speed of motion; Likewise, they are very useful to suggest the possible mechanisms that take place in the removal process. The most and herby used models are the Lagergren pseudo-first-order (PFO, Eq. (4)), Ho & Mckay pseudo-second-order (PSO, Eq. (5)), and Elovich kinetic model (Eq. (6)).

$$\log(q_e - q_t) = \log(q_e) - \frac{k_1}{2.303}t \cdots \tag{4}$$

$$\frac{t}{q_t} = \frac{1}{k_2 q_e^2} + \frac{t}{q_e} \cdots \tag{5}$$

$$q_t = \frac{1}{\beta}\ln(\alpha\beta) + \frac{1}{\beta}\ln(t) \cdots \tag{6}$$

where q_e is the amount of drug sorption at equilibrium (mg·g^{-1}), q_t is the amount of drug sorption at a given time *t* (mg·g^{-1}), k_1 the equilibrium rate constant in the pseudo-first-order model (min^{-1}), k_2 the constant equilibrium rate of the pseudo-second-order model (g·mg^{-1}·min^{-1}), *h* ($k_2 q_e^2$) the primary sorption rate, α the initial adsorption rate (mg·g^{-1}·min^{-1}), and β the desorption constant (g·mg^{-1}).

Other factors involved in the adsorption process were evaluated using the equation (7) for the intraparticle diffusion model and the equations 8–10 for the Boyd diffusion models.

$$q_t = K_{id}\sqrt{t} + C_{id} \cdots \tag{7}$$

$$F = 1 - \left(\frac{\pi^2}{6}\right)\exp(-B_t) \cdots \tag{8}$$

$$F = \frac{q_t}{q_e} \cdots \tag{9}$$

$$B_t = -0.4977 - \ln(1 - F) \cdots \tag{10}$$

where K_{id} (mg/g·min$^{1/2}$) is the model rate constant, C_{id} the model constant, *t* and B_t are mathematical functions of *F*.

Additionally, the initial adsorption factor (R_i) of the intraparticle diffusion model was evaluated using the equation (11).

$$R_i = \frac{q_{ref} - C_{id}}{q_{ref}} = 1 - \left(\frac{C_{id}}{q_{ref}}\right) \cdots \tag{11}$$

The last expression represents R_i as the ratio of the initial adsorption amount (C_{id}) to the final adsorption amount q_{ref}.

2.7. Determination of molecular electrostatic potential (MEP)

Additionally, for further explanation of how the drugs interact with the biosorbent, the Molecular Electrostatic Potential (MEP) on the electron density surface of each drug was plotted by means of a DFT calculation using Gaussian 16 and later analyzed using GaussView 6 (Frisch et al. 2016). Geometry was fully optimized, assuming an ultrafine numeric integration

cell, no symmetry restrictions, a temperature set at 278 K in the presence of water; using the range-separated functional ωB97XD, with the 6–311 g(d,p) basis sets and CPCM as the Self-Consistent Reaction Field (SCRF) method. Simulation conditions were maintained at every step of re-optimization, while convergence in force/displacement parameters in numeric and analytical hessian ensured a local energy minimum in the final structures.

2.8. Sargassum characterization

The *Sargassum* was characterized before and after the removal of the drugs. Diverse techniques were used to evidence the changes in the algae due to the presence of the drugs. The functional groups from *Sargassum* organic compounds and the changes caused by the presence of the drugs were evaluated by FTIR analysis. The spectrum was recorded from 400 to 4000 cm^{-1} using a Spectrum Two FTIR spectrometer (Perkin Elmer, Waltham, MA, United States). Crystalline phases and structural changes in *Sargassum* were evaluated by X-ray diffraction using a Rigaku Ultima IV diffractometer with Cu Kα radiation in a range of 20 to 80°. The dry *Sargassum* samples were placed in copper sample holders and coated with gold for microscopy analysis. A SEM/STEM Hitachi SU8230 cold-field emission scanning electron microscope (Hitachi High-Tech, Tokyo, Japan) was employed to determine the *Sargassum* morphology. The chemical analysis was evaluated using an energy-dispersive X-ray spectrometer XFlash 6/60. Finally, a TGA/DSC Model 2 + StaRe System (Mettler-Toledo Intl. Inc., Columbus, OH, USA) thermal analyzer was used to determine the concentration of PCT, DFS, or IBU under a controlled nitrogen atmosphere. The analysis was performed from 30 to 700 °C using a 10 °C/min rate.

3. Results

3.1. Removal of drugs

The monitoring of drug removal was carried out by fluorescence analysis using quantum dots (CDs), which are fluorescent materials with quasi-spherical form and are approximately 10 nm in size. CDs have been commonly used in a broad range of applications, including drug delivery (Yuan et al. 2017), bioimaging (Damarla et al. 2020), photocatalysis (Fernando et al. 2015), and as sensors (Cui et al. 2017) due to their unique optical properties, high photostability, low toxicity, biocompatibility, and inexpensive nature. Fluorescent sensors are often used to detect many ions owing to their simplicity and sensitivity. In the case of CDs, one of the most accepted fluorescence mechanisms is defined by their surface state, including the degree of oxidation and functional groups. By this mechanism, the protonation and deprotonation of the functional groups could result in the quenching/enhancement of CDs' fluorescence.

The quenching-based drug detection feasibility was first assessing the interactions of CDs with each drug. DFS, IBU, and PCT concentrations from 0 to 15 ppm were mixed with 50 µg/mL of CDs to perform the calibration curve. Each solution was illuminated at 360 nm to excite the CDs and record their fluorescence spectra. Then, the analysis was centered at 480 nm because a higher fluorescence intensity was found there

for each sample. Fig. 1a presents the calibration curves obtained after normalization. As can be noticed, the concentration is directly proportional to the fluorescence intensity, causing an enhancement in the fluorescence emission; therefore, the quantification of each drug could be made by monitoring fluorescence intensity variations.

Taking advantage of this process, while the *Sargassum* removed each drug from water, every 10 min was taken a sample, mixed with 50 µg/mL of CDs, and analyzed through fluorescence. Again, the excitation wavelength was fixed at 360 nm and the emission wavelength at 480 nm to quantify the remotion efficiency using the calibration curve previously obtained. Fig. 1b shows the amount of each drug removed against time, where a decrease of each drug concentration is observed in each experiment, confirming the capabilities of the *Sargassum* to remove this kind of contaminants. The test was repeated three times, and in each one the remotion efficiency was around 98 % of DFS, 85 % of IBU, and 54 % of PCT with a standard deviation of 0.63 %, 0.77 %, and 0.84 %, respectively. As can be seen, DFS shows a more considerable remotion, followed by IBU and PCT. Then, it is easier for the *Sargassum* to adsorbed DFS and more difficult for PCT.

Changes in the sorption capacity of *Sargassum* against time are presented in Fig. 2a; as it is observed, as time increases, the drug sorption from the algae increases. The remotion takes place rapidly for DFS and IBU during the first 20 min of the experiment, while PCT uptake is more constant through time until all reach the equilibrium found at 120 min. The values obtained for sorption capacity coincide with the percentage of removal in equilibria since DFS sorption has both the highest removal ($R = 98$ %) and the highest sorption capacity ($q_e = 2.4677$). In contrast, PCT has the lowest removal ($R = 54$ %) and sorption capacity ($q_e = 1.4151$), and IBU is in between ($R = 85$ %, $q_e = 2.0842$). Furthermore, the remotion values are higher than those from other algae and microalgae reported elsewhere (Coimbra et al. 2018, Santaeufemia et al. 2018, Parus et al. 2020, Hifney et al. 2021). For example, in this work, the maximum adsorption capacities were approximately-two times less IBU than Santaeufemia et al. (Santaeufemia et al. 2018) (3.97 mg vs 1.7 mg), the same amount of PCT as Parus et al. (Parus et al. 2020), and five times the maximum adsorption capacities of DFS attained by Hifney et al. (0.429 mg vs 2.3 mg) per gram of algae. It is important to notice that the sorption capacity values obtained from fluorescence analysis with CDs are consistent and have similar values to those obtained from TGA analysis. Thus, the latest can be a handy tool when other characterization techniques for measuring drug removal such as HPLC are unavailable.

On the other hand, the capability of reusing the *Sargassum*, four cycles of remotion were performed with each drug, and the results are shown in Fig. 2b. As can be seen, even when the efficiency is lower, even after three cycles, the remotion of DFS and IBU reaches around 60 %. This implies that some active sites or pores remain occupied between each cycle, then the concentration of each drug is higher enough to totally saturate the active sites at a lower concentration than the previous cycle.

One of the parameters that can favor the biosorption of some pollutants is the temperature of the system. The Fig. 3 shows the removal of DFS, IBU, and PCT at different temperatures. As can be seen, the removal of drugs is favored when
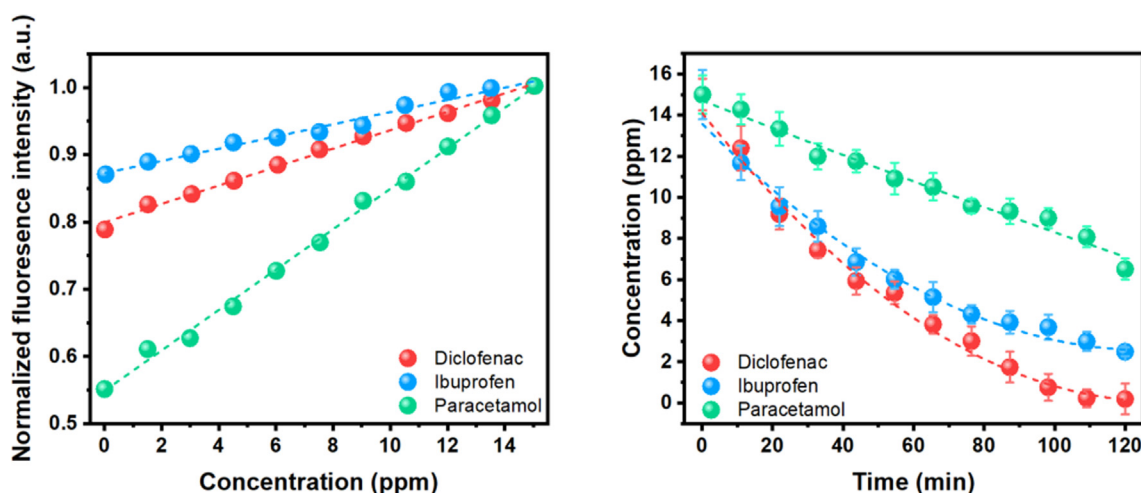
Fig. 1 a) Calibration curves to quantify DFS, IBU, and PCT concentrations. b) Effect of contact time on removing DFS, IBU, and PCT. Conditions: temperature (25 °C), pH (6), algal concentration (6 mg·mL^{-1}), and initial drug concentration (15 ppm).

the temperature is increased to 30 and 40 °C. For the three drugs, 100 % removal is obtained with increasing temperature. This behavior has been previously reported (Khadir et al. 2020, Wu et al. 2021), showing that drug biosorption is an endothermic process. However, according to Sajid et al. (Sajid et al. 2022), the increase in high temperatures can become an exothermic process, decreasing their removal.

Previous results show that drug removal using sargassum as biosorbent material is an efficient process, even at room temperature. In this sense, different materials and processes have been used for the same purposes. Table 1 shows a compilation of various recent works in which the removal of drugs was carried out. As can be seen, in most reports, removal efficiency is

high, in some very close to 100 %. However, in some cases sophisticated materials such as composites or nanostructures were used, whose synthesis is a complex process. Among the most used removal methods are adsorption and photodegradation. In addition, depending on the type of process, conditions such as temperature, pressure and energy are required. It should be noted that in this work the biosorbent material is a dead algae and the removal process does not require specific conditions. In addition, the use of sargassum is of great importance in some parts of the world, specifically on the coasts of the Caribbean Sea, due to the overpopulation of this algae in recent years, which has brought serious environmental and economic problems.

Table 1 Reported works for the removal of DFS, IBU, and PCT using various materials and processes.

| Drug	Material	Process	Efficiency	Reference
Paracetamol				
	Iron and aluminum electrodes	Electrocoagulation	78	(Negarestani et al. 2020)
	Activated carbon	Adsorption	50	(Sajid et al. 2022)
	Organic iron(III) complexes	Photodegradation	47	(Benssassi et al. 2021)
	Chlorella sorokiniana microalgae		41	(Escapa et al. 2017)
	ZnO supported on polystyrene pellets	Photodegradation	77	(Vaiano et al. 2018)
	CNT-COOH/MnO2/Fe3O4 nanocomposite	Adsorption	94	(Lung et al. 2021)
Ibuprofen				
	TiO2/Activated carbon	Photodegradation	93	(Conde-Rivera et al. 2021)
	Iron and aluminum electrodes	Electrocoagulation	48	(Negarestani et al. 2020)
	TiO2/Activated carbon	Photodegradation	~92	(Gu et al. 2019)
	Cu-doped Mil-101(Fe)	Adsorption	56	(Xiong et al. 2021)
	Cellulosic sisal fibre/polypyrrole-polyaniline nanoparticles	Adsorption	88	(Khadir et al. 2020)
	Biomass fiber/β-CD/Fe3O4	Adsorption	90	(Wu et al. 2021)
Diclofenac				
	Activated sludge	Adsorption	98	(Elshikh et al. 2022)
	Carbonaceous aerogel honeycomb monolith	Adsorption	84	(Puga et al. 2021)
	Reduced graphene/copper oxide nanocomposites.	Adsorption	97	(Moradi et al. 2022)
	H2-based membrane biofilm reactor with Pd nanoparticles	Catalytic reductive dechlorination	95	(Liu et al. 2022)
	Chitosan/iron nanoparticles composite	Adsorption	85	(Alothman et al. 2020)
	MgAl layered double hydroxide	Adsorption	65	(Mkaddem et al. 2022)
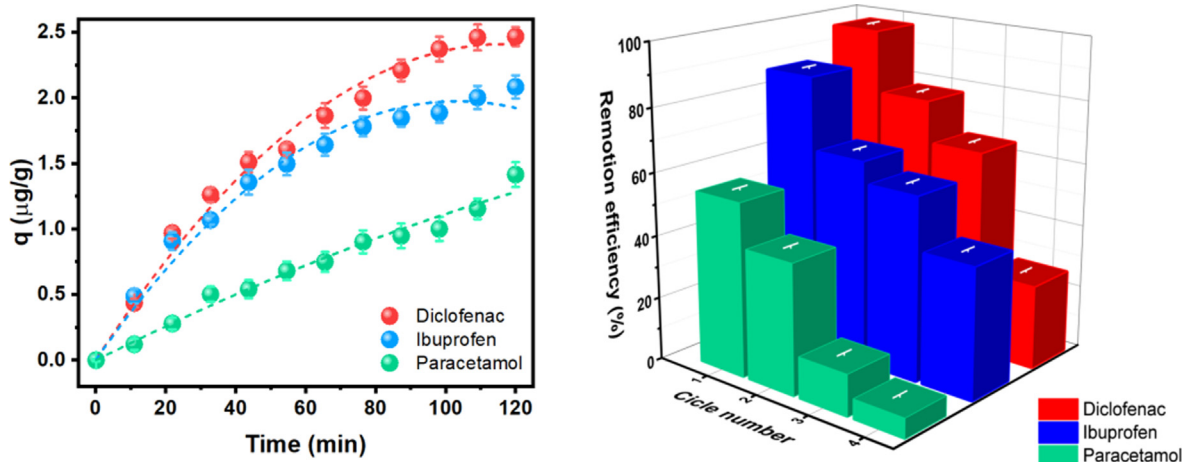
Fig. 2 a) Time-dependent removal capacity for DFS, IBU, and PCT. b) Recycling (reuse) of *Sargassum*; change in remotion efficiency (%) after four cycles of the selected drugs at 25 °C.
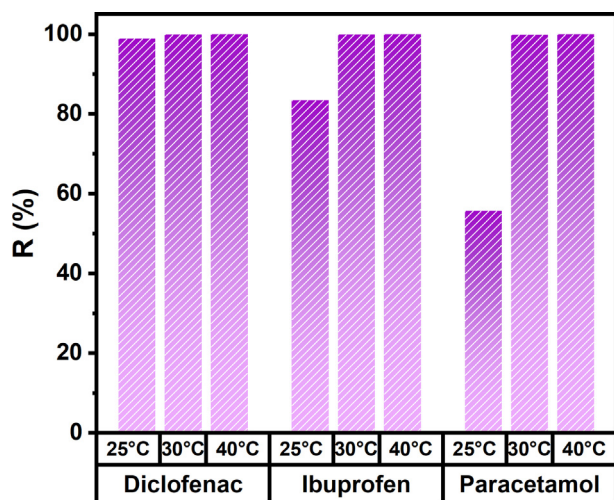

Fig. 3 Removal percentage of DFS, IBU, and PCT at different temperatures (25, 30, and 40 °C).

3.2. Analysis of drugs biosorption

Differences between the remotion of DFS, IBU, and PCT may be related to the physical properties and chemical affinity among the molecules and the biochemical composition of the algae cell wall. A distribution coefficient (sometimes so-called partition coefficient) is widely used to relate the concentration of a chemical solute in a specific phase related to that in another between which equilibrium is approached. The solute can be any inorganic/organic substance, and the phase of interest can be any media such as water, air, soil, sediment, etc. This parameter is often used in drug design as a proxy measure for membrane permeability.

The values of K_d are of great interest since they can be related to the biosorption of *Sargassum* from the perspective of their functional groups. *Sargassum's* cell wall possesses a wide variety of functional groups, such as carboxyl, sulfhydryl, and hydroxyl, that could act as binding sites for the selected

drugs (as already discussed from the FTIR analysis), and Fig. 4 shows the data obtained from K_d for each of the selected drugs. It is observed that there exist different behaviors of distribution coefficient for each drug against time; its values at the equilibrium time are consistent with the tendency obtained from both removal and sorption capacity (S-DFS > IBU > PCT). For PCT, it is observed that practically K_d is constant against time. This behavior is an indication that the drug does not interact entirely with the functional groups in the cell wall of the brown algae; unlike DFS, at the begging of the sorption K_d is constant. Still, after 80 min, an exponential increase reflects a higher drug interaction with the cell wall. It has been recently proposed that calcium is necessary for maintaining the fibrous layer in the cell walls of brown algae, composed mainly of alginate gels (Terauchi et al. 2016).

Differences between DFS, IBU, and PCT remotion may be related to physical properties, the chemical affinity among the
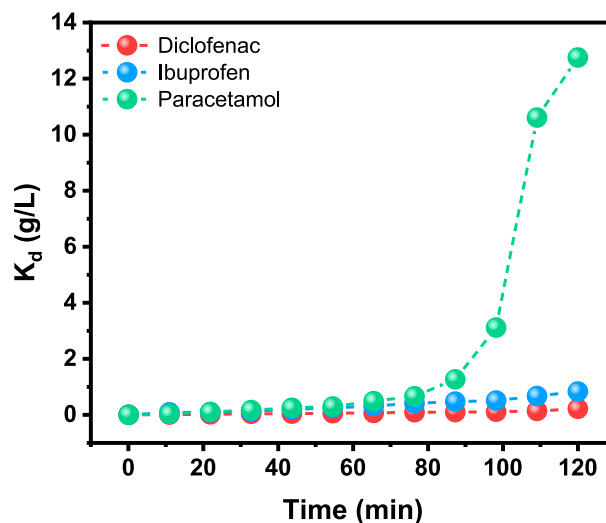

Fig. 4 Distribution coefficient K_d obtained vs time of DFS, IBU, and PCT.

molecules, and the biochemical composition of the algae cell wall. Besides, it is known that pH alters the surface charge of the adsorbent due to functional group dissociation. Even more, the remotion is also influenced by the acid-base dissociation constant, pKa, defined as the pH at which the drug is 50 % ionized. Thus, to better understand the mechanism behind the remotion and efficiency between each contaminant, the remotion was evaluated by changing the pH of the DFS, IBU, and PCT solutions at 3.0, 4.0, 7.0, and 9.0. Then each solution was put in contact with *Sargassum* to evaluate the remotion.

Interestingly, the curves did not show important variations against pH, suggesting that the *Sargassum*, with all their functional groups, acts as a buffer that could maintain a stable pH in the peripheral solution without limiting the remotion efficiency. Thus, the pH of the solution was measured, resulting in pH = 6 in the three systems, corroborating the suggestion. Using absorbents with a negative charge, some researchers have reported that the adsorption efficiency of DFS decreases at pH values below its pKa (4.2) because it presents a neutral form. However, it carries a negative charge at pH values higher than 4.2. Additionally, sodium ions from DFS present an electrostatic interaction with carboxyl groups, resulting in higher adsorption efficiency at pH 6 (Hifney et al. 2021). Comparably, IBU is not charged at low solution pH, equal to or below to pKa (4.9). However, as the solution pH increases, the carboxylic group begins to dissociate. Almost all IBU molecules are negatively charged when the solution pH is above 7 (Santaeufemia et al. 2018), explaining why we have better remotion efficiency of DFS than IBU, even when their pKa is similar. In contrast, PCT has a pKa value between 9.0 and 9.50 (Parus et al. 2020). Therefore, solutions with 2.0 < pH < 9.0 present neutral PCT molecules, limiting the remotion by chemical means, suggesting a physical remotion.

3.3. Kinetic analysis of the drugs removal

The use of adsorption kinetics parameters can help to predict, evaluate and understand the sorption rate; it gives relevant information on the properties of the adsorbent for the target pollutants for assessing, designing, scaling, and modeling the process. Sorption kinetics are described by different models, where time-dependent changes in the adsorbate concentration until an equilibrium state is reached are observed. Therefore, the adsorption of the various drugs was fitted using the Pseudo First Order (PFO), Pseudo Second Order (PSO), and Elovich kinetic models; the kinetic parameters obtained from the described models are depicted in Table 2, and their correct fit to the experimental data was compared using the correlation values (R^2).

The PFO kinetic model assumes that the sorption rate is proportional to the number of surface vacancy sites on the adsorbent (Borhan et al. 2019). The PSO kinetic model assumes that the sorption rate is linearly related to the square number of the vacancy sites available on the adsorbent (Borhan et al. 2019). Finally, the Elovich kinetic model describes activated chemical adsorption, assuming that the system has energetically heterogenous adsorbing surfaces; in other words, the adsorption rate decreases exponentially as the surface coverage increases by the adsorbent (Wu et al., 2009a), (Sahoo and Prelot, 2020).

Table 2 Kinetic parameters for removing DFS, IBU, and PCT by the brown algae *Sargassum* using an initial concentration of 6 mg·mL^{-1} of biomass.

Kinetic model	Drug		
	DFS	IBU	PCT
Pseudo First Order (PFO)			
Experimental q (q_e)	2.47	2.08	1.42
Model q (q_{cal1})	4.63	2.68	1.54
k_1	0.04	0.03	0.01
r^2	0.74	0.96	0.97
Pseudo Second Order (PSO)			
Experimental q (q_e)	2.47	2.08	1.42
Model q (q_{cal2})	4.36	2.12	7.60
k_2	0.01	0.01	0.01
h	0.05	0.07	0.01
r^2	0.96	0.96	0.19
Elovich			
β	1.13	1.78	2.04
α	0.12	0.16	0.04
r^2	0.98	0.92	0.90

The kinetics results showed that all the drugs are consistent with different kinetics models, as observed from the relation coefficient (R^2) obtained for each. It is observed that in all drugs R^2 for the Elovich model are relatively high (> 0.9). In particular, DFS presents the highest value (0.9842), suggesting that this model best represents its adsorption kinetics. For the PFO model, the correlation values for IBU and PCT (0.9570 and 0.9662, respectively) are reasonably good, indicating that the model described the results better than the Elovich model. Finally, the R^2 values for the PSO model from DFS and IBU (0.9646 and 0.9612, respectively) are pretty high to fit the model of both drugs' adsorption by *Sargassum*. As observed, IBU is well fitted by the PFO and PSO models, but when analyzing the derivate q_{cal2} from the PSO is observed, it is closer to the experimental data q_e than the q_{cal1} from PFO model, suggesting the PSO model describes IBU kinetics.

In summary, S-PCT is governed by the PFO kinetic model, suggesting mainly surface adsorption and is consistent with the fact the K_d behavior, discussed in Fig. 4, has the lowest value and is almost constant through time, indicating no chemical interaction. S-IBU agrees with the PSO and may be explained on the assumption that its rate-limiting step, as chemisorption, involves valency forces through sharing or exchanging electrons between adsorbent and adsorbate (Jellali et al. 2011, Riahi et al. 2017); which also explains why K_d evolution through time is slow but has a higher equilibrium value than S-PCT. Finally, the data for S-DFS had a good agreement with the Elovich model; this involves a variation of the energies in the chemisorption with the active sites that are heterogeneous in *Sargassum* and therefore exhibit different activation energies for chemisorption because of cell walls composition (Riahi et al. 2017) and has consistency with the results obtained from K_d.

These results imply that the chemisorption mechanism may play an essential role in the adsorption of DFS and IBU by *Sargassum* and are consistent with other studies (Coimbra

et al. 2018, Santaeufemia et al. 2018, Parus et al. 2020, Hifney et al. 2021). For PCT is implied that adsorption occurs mainly by diffusion through the *Sargassum* interface (Krstić 2021). Despite these suggestions, the good fitting of the models for the rest of the drugs indicates that *Sargassum* is a highly heterogeneous system in which surface adsorption, chemisorption, and probably ion exchange, intraparticle diffusion, and precipitation co-occur.

Further analysis of the factors limiting the adsorption process, the adsorption curves of the different NSAIDs over time were fitted by intraparticle diffusion (eq. (7)) and the Boyd diffusion (eq. 8–10) models, as observed in Table 3.

Generally, the adsorption process is affected by both intraparticle/film diffusion, and more information on the mechanism involving the Sargassum in the presence of the different NSAIDs can be obtained by determining the rate-controlling step by using the proposed models. The results related to intraparticle and film diffusion can be observed in Table 3. It is observed that S-DFS and S-IBU have an excellent linear correlation with intraparticle diffusion. In contrast, S-PCT has a linear correlation with Boyd's diffusion model, showing a different description of the adsorption process as already observed kinetics. It is observed in both cases a single, main controlling and rate-limiting stage of adsorption which can be related to slow adsorption in which the adsorption sites are bit by bit occupied, and the NSAID number increase inside Sargassum. During the process, differences between the potential energy and the NSAID in the solution gradually decrease or even exceeds the potential energy of the solution, so the adsorption rate is low in which a dynamic equilibrium cannot be reached before the drug completely occupies the adsorption sited. Moreover, from Table 3, the intercept of the fitting line is not 0 on the Y-axis in both models. It is shown that neither was the only rate-controlling step, and adsorption may be controlled by many factors (Shang et al. 2021) but mainly intraparticle diffusion for S-DFS and S-IBU, and film diffusion for S-PCT.

Additionally, the adsorption process can be further analyzed using an expression described by (Wu et al., 2009b), which after mathematical rearrangement can give a term defined as the initial adsorption factor (R_i) of the intraparticle diffusion model (equation (11)). The R_i values obtained for the adsorption of the NSAID onto de *Sargassum* are 0.92 for S-DFS, 0.94 for S-IBU, and 0.84 for S-PCT. These results suggest that the R_i values for S-DFS and S-IBU are under zone 1 regiment in which weak initial adsorption takes place. S-PCT

is under zone 2, meaning initial intermediate adsorption (Wu et al., 2009b, Pholosi et al. 2020). With the obtained data, it can be suggested that surface adsorption is not the dominant process as already described since *Sargassum* is a very heterogeneous matrix for the adsorption process of the NSAID.

3.4. Molecular electrostatic potential (MEP)

These observations are further confirmed by observing the MEP analysis of the drugs in the presence of water (pH 6), as seen in Fig. 5. MEP is an important study in molecule interactions since it can predict relative sites for nucleophilic and electrophilic attacks. The electrostatic surface potentials are presented using different colors. By convention, red is used for negative (electrophilic reactivity), green for zero, and blue for positive (nucleophilic reactivity) electrostatic potentials.

For DFS, it is observed that the molecule, in general, is slightly negatively charged, and the most negative electrostatic potential is localized in the carboxylate ion. For IBU, the molecule is more neutral charged (and thus has higher intermolecular interactions). The most negative potential is located on the carbonyl group's oxygen molecule, which is next to a positive potential from the hydrogen in the hydroxyl group of the carboxyl. PCT has two positive potential regions in the aminophenol molecule, one from the hydrogen of the hydroxyl group and the other from the hydrogen of the nitrogen group, besides a slight negative potential from the oxygen present in the acetyl substituent of the amino molecule. These red regions in all drugs are potential sites for an electrophilic attack. When comparing the energy values obtained from MEP (DFS = $|6.69|eV$, IBU = $|179.74|eV$ and PCT = $|212.24|eV$) considering calculations using water as a solvent, it is clear that DFS has the highest probability of an electrophilic attack since it has the lowest absolute energy value. In contrast, IBU and PCT have lower probability (lower absolute energy). These results can be related to pH, which is an important factor for the K_d values between *Sargassum,* drugs, the remotion, and the sorption capacity of *Sargassum* to these selected drugs.

3.5. Characterization of Sargassum

The *Sargassum* used for the drugs removal was recovered and dried to analyze it by the different characterization techniques and, in this way, determine the changes suffered during the removal of the drugs. X-ray diffraction (XRD) was used to identify the structures present in the pure *Sargassum* (S) and the *Sargassum* with absorbed IBU (S-IBU), DFS (S-DFS), and PCT (S-PCT) drugs. Fig. 6a shows the XRD patterns, confirming the presence of calcium carbonate "calcite" ($CaCO_3$) ICDD 00–005-0586, magnesium sulfide "iningerite" (MgS) ICDD 00–035-0730, and calcium oxalate hydrate ($C_2H_{4.5}CaO_{6.25}$) ICD 00–020-0233 phases in all the samples. It is important to mention that, unlike other reports (Paraguay-Delgado et al. 2020), in this particular case, the calcium oxalate phase was found in the pure *Sargassum* samples. However, this phase was removed when drugs were absorbed, decreasing the intensity of the peaks. This can be related to a change in the cell wall integrity of the *Sargassum* (Terauchi et al. 2016). In contrast, the intensity of the diffraction peaks of the calcium carbonate phase increases, which means a higher

Table 3 Diffusion parameters obtained from the removal of drugs.

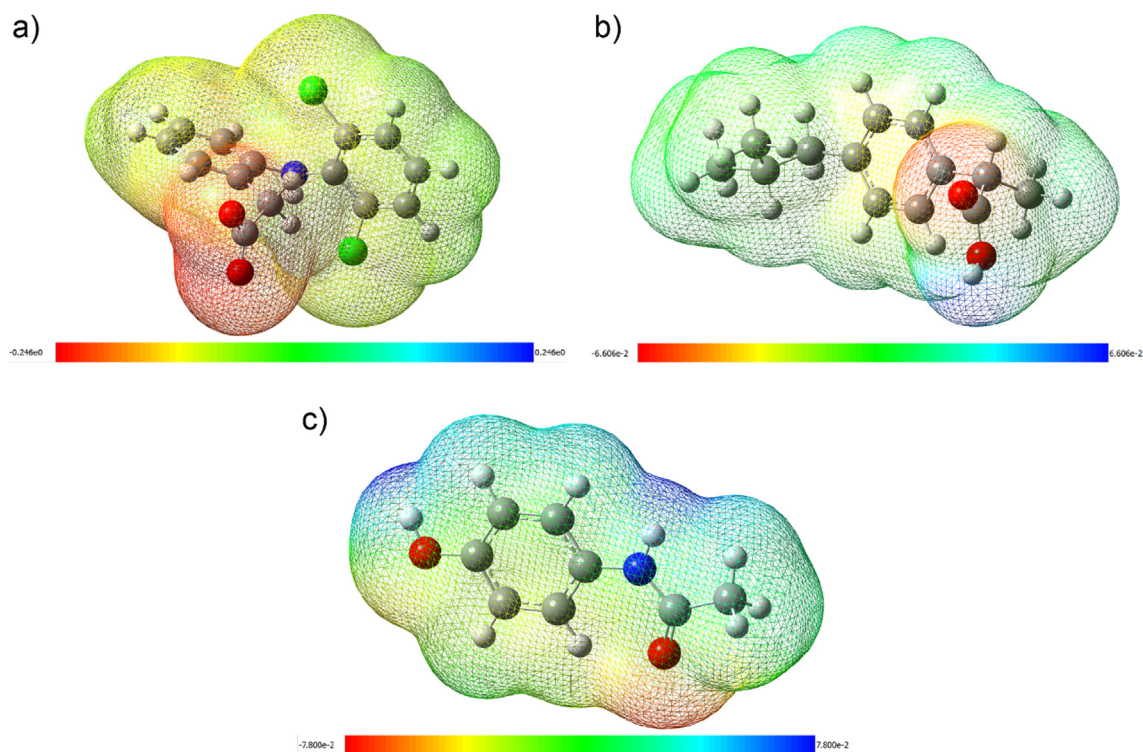| Diffusion model	NSAID		
	DFS	IBU	PCT
Intraparticle Diffusion			
K_{id}	0.25	0.19	0.13
C_{id}	0.20	0.06	0.23
R_i	0.92	0.97	0.84
R^2	0.99	0.98	0.93
Boyd's Diffusion			
y-intercept	−1.13	−0.51	−0.58
R^2	0.74	0.96	0.97

Fig. 5   Schematic representation of MEP surfaces of a) DFS, b) IBU, and c) PCT.
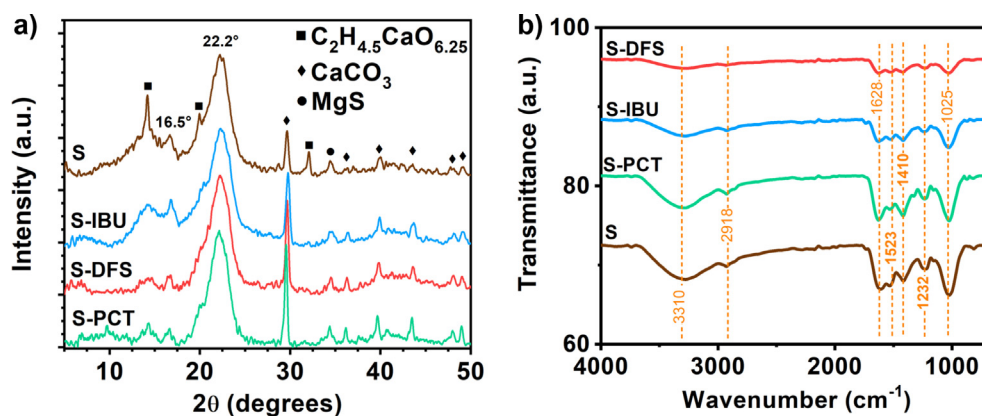

Fig. 6   Characterization of *Sargassum* before and after the removal of drugs: a) XRD patterns, and b) FTIR spectra.

concentration in the samples, while the MgS phase is almost the same in all the samples. There are two diffraction peaks at 2θ values, 16.5°, and 22.2°, which are characteristic peaks of the alginate phase coming from the *Sargassum* (Helmiyati and M. Aprilliza, 2017), Kavitha et al. 2019). Considering the peak height intensity and the degree of crystallinity could diagnose the semi-crystalline nature of alginate (Dalal et al., 2021a). In addition, the structure of the diatoms, which is a random network of tetrahedral bond silicon atoms, is localized mainly between 2θ values 20° to 25° (Briceño et al. 2021). The diffraction peaks of the drugs are predominantly found at 2θ values lower than 25°. Slight differences can be observed in the XRD patterns between 2θ values 5 to 15°, which correspond to the effect of the different drugs compared to pure *Sargassum*.

An FTIR analysis was carried out to support the results obtained by XRD. Fig. 6b shows the FTIR spectra of *Sargassum* before and after removing each of the drugs. Various signals can be observed in the spectrum corresponding to *Sargassum*. The strong band located at 3310 cm^{-1} corresponds to the O—H bond of the hydroxyl groups of the aromatic compounds from the *Sargassum*. This type of compound is corroborated by the vibrations from the aromatic rings observed at 1523 cm^{-1}. The presence of non-aromatic compounds in *Sargassum* is demonstrated by the vibration at 2900 cm^{-1}, corresponding to C—H groups. The band centered at 1628 cm^{-1} corresponds to COO vibrations from metal carboxylates and C=O bonds from alginates (Samir et al. 2016, Dalal et al., 2021a). The signal at 1410 cm^{-1} is attributed to the vibrational band of the C—O group of calcite present in this type of algae

(Paraguay-Delgado et al. 2020). The sulfates in brown algae, contained mainly in fucoidan, have been previously reported (Sinurat et al. 2016). In this case, the signals located at 1230 cm^{-1} and 832 cm^{-1} confirm the presence of S—O groups. Finally, the band located at 1030 cm^{-1} is attributed to the C—O groups coming from the alginates in the *Sargassum*. By comparing the spectra, the same bands can be observed, with intensities variations due to the interaction of the drugs with the organic compounds of the *Sargassum*. Mainly, a notable decrease in intensity is observed in the band corresponding to the O—H group (3200 cm^{-1}), which can also be observed in the bands centered at 1628 cm^{-1} (C=O) and 1030 cm^{-1} (C—O), suggesting that O—H bonds are involved in the drug biosorption process.

The surface morphology of the pure *Sargassum* and S-IBU, S-DFS, and S- PCT was observed by scanning electron microscopy (SEM), displayed in Fig. 7. Fig. 7a shows the SEM images of the pure *Sargassum* where the surface morphology is irregular. Even diatoms, found in almost marine water with a siliceous skeleton, are presented. Also, besides diatoms, calcium oxalates were found. As mentioned in the methodology section, the samples were washed to eliminate waste from the marine environment; however, some structures are still present. Fig. 7b, 7c, and 7d show a totally different surface morphology than pure *Sargassum*. All the SEM images clearly show fibrils characteristic of alginate (Helmiyati and M. Aprilliza, 2017). In addition, some impurities have been removed because of the effect of the drugs, such as calcium oxalate; however, diatoms and calcium carbonate structures can still be observed. Fig. 7e shows the EDS spectra of the samples. As can be noted, all the spectra show calcium (Ca), sulfur (S), magnesium (Mg), oxygen (O), and carbon (C)

elements from the *Sargassum*. Gold (Au) and aluminum (Al) elements are from the thin metallic coating and the holder used in the analysis, respectively. It is interesting to notice that the silicon (Si) element is present in all the samples, which is part of the structure of diatoms, indicating the presence of these structures in all samples.

The presence and concentration of drugs can also be estimated by thermogravimetric analysis. Fig. 8a shows the TGA results obtained. The dry *Sargassum*, free of drugs (S), was subjected to treatment observing three different processes. In the range between 30 and 200 °C, a weight loss is observed, attributed to the evaporation of the water present in the *Sargassum*. Afterward, the decomposition and calcination of organic compounds occur between 200 and 600 °C, observing a significant decrease in weight. Finally, the event between 600 and 700 °C corresponds to the generation of CO_2 due to the decomposition of carbonates. Previous studies have already reported this behavior in this type of algae (Paraguay-Delgado et al. 2020, Alzate-Gaviria et al. 2021). At the end of the experiment, a remaining weight of 32.5 % is observed. This means that *Sargassum* loses 67.5 % of its weight. Subsequently, the *Sargassum* samples containing each drug were subjected to the same analysis. The results indicated a percentage of the remaining weight of 32.55 %, 32.58 %, and 32.59 % for PCT, IBU, and DFS, respectively (inset in Fig. 8a). In this way, it was estimated that the amount of DFS, IBU, and PCT per gram of *Sargassum* was 2.77, 2.46, and 1.54 mg, respectively.

On the other hand, the decomposition of these types of drugs by TGA analysis has been determined by the derivation process of the curve obtained (Higareda et al. 2019). Specifically, the second derivative has been used for these purposes,
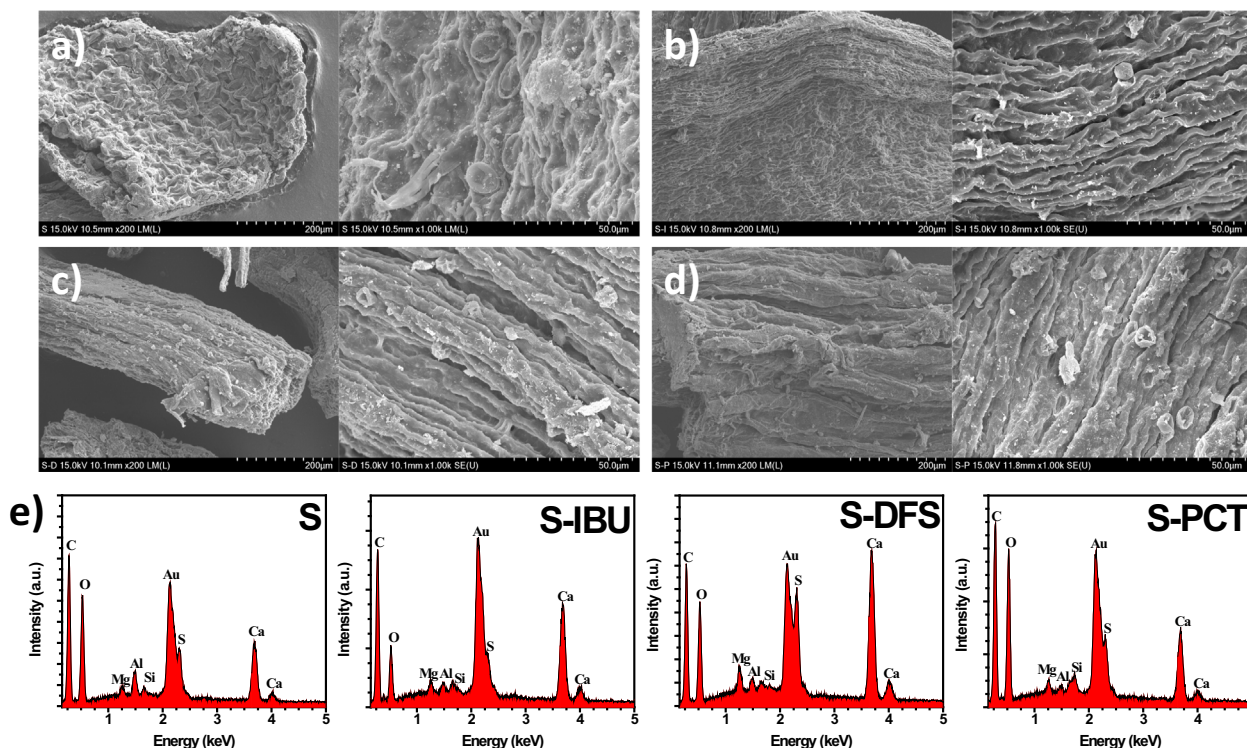

Fig. 7 SEM images of a) pure *Sargassum*, b) S-IBU, c) S-DFS, d) S-PCT, and e) EDS spectra of the samples.
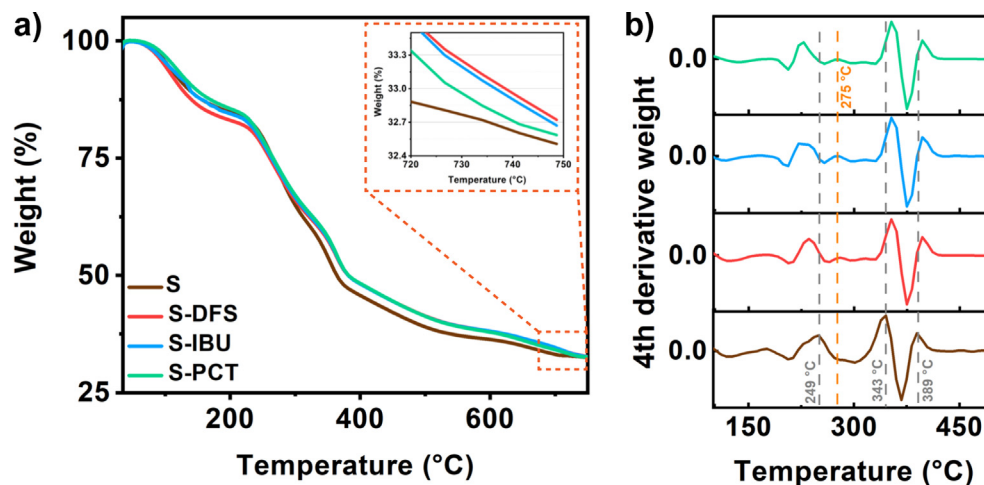
Fig. 8 a) Thermogravimetric analysis and b) Four derivative weight plots of *Sargassum* before and after the drug's removal.

finding a peak between 250 and 300 °C. However, in this study, it was not possible to distinguish this signal due to the similarity between the composition of the *Sargassum* and the drugs. Therefore, the fourth derivative analysis was carried out, shown in Fig. 8b. As can be seen, in the curve corresponding to *Sargassum*, there are three peaks or intense signals located at 249, 343, and 389 °C due to the decomposition of organic compounds. These same signals can be observed in the curves corresponding to *Sargassum* containing the different drugs. However, shifts to the left are noticeably observed because of PCT, DFS, or IBU. Furthermore, an additional signal is observed between 260 and 290 °C, attributed to drug decomposition, as previously reported (Khanmohammadi et al. 2012, de Oliveira et al. 2017). These results corroborate the biosorption of drugs in the *Sargassum*.

4. Conclusions

The present work demonstrated the biosorption capacity of *Sargassum* to remove some drugs dissolved in water. The drugs evaluated were DFS, IBU, and PCT, whose use was notably increased during the period of the COVID-19 pandemic. The removal percentages are comparable to or even higher than those achieved by other types of removal systems. DFS was the drug that was removed to a greater extent (98 %), while IBU and PCT were removed by 85 and 54 %, respectively. These removal percentages were corroborated by TGA analysis, determining the drug concentration in the *Sargassum*. The high rate of DFS removal should be noted, which has been challenging to remove by other methods.

In addition, the removal of the drugs was not susceptible to changes in pH because the organic compounds from the *Sargassum* maintained the system in an acid condition. On the other hand, *Sargassum* can be reused without affecting its biosorption efficiency for three cycles and without affecting its removal capacity. The biosorption of these drugs depends largely on their properties, such as polarity and composition. The biosorption mechanism occurs in different stages and follows various kinetic models because of the interaction between drugs and certain organic compounds of *Sargassum* SEM characterization demonstrated morphological changes in *Sargassum* due to drug biosorption. Therefore, the use of *Sargassum* represents an alternative for removing drugs, being highly effective, simple, economical, and friendly to the environment.

Declaration of Competing Interest

The authors declare that they have no known competing financial interests or personal relationships that could have appeared to influence the work reported in this paper.

Acknowledgement

References

Ademollo, N. et al, 2021. Occurrence, distribution and pollution pattern of legacy and emerging organic pollutants in surface water of the Kongsfjorden (Svalbard, Norway): Environmental contamination, seasonal trend and climate change. Mar. Pollut. Bull. 163, 111900.

Alothman, Z.A. et al, 2020. Synthesis of chitosan composite iron nanoparticles for removal of diclofenac sodium drug residue in water. Int J Biol Macromol 159, 870–876.

Alzate-Gaviria, L. et al, 2021. Presence of Polyphenols Complex Aromatic "Lignin" in Sargassum spp. from Mexican Caribbean. Journal of Marine Science and Engineering 9 (1).

Awoyemi, M.O. et al, 2021. Water and sub-soil contamination in the coastal aquifers of Arogbo, Ondo State, Nigeria. J. Hydrol.: Reg. Stud. 38, 100944.

Barcelo, D., 2020. An environmental and health perspective for COVID-19 outbreak: Meteorology and air quality influence, sewage epidemiology indicator, hospitals disinfection, drug therapies and recommendations. J. Environ. Chem. Eng. 8, (4) 104006.

Benssassi, M.E. et al, 2021. Removal of paracetamol in the presence of iron (III) complexes of glutamic and lactic acid in aqueous solution under NUV irradiation. Sep. Purif. Technol. 261, 118195.

Bimová, P. et al, 2021. Biochar–An efficient sorption material for the removal of pharmaceutically active compounds, DNA and RNA fragments from wastewater. J. Environ. Chem. Eng. 9, (4) 105746.

Bonnefille, B. et al, 2018. Diclofenac in the marine environment: a review of its occurrence and effects. Mar. Pollut. Bull. 131, 496–506.

Borhan, A. et al, 2019. Characterization and Modelling Studies of Activated Carbon Produced from Rubber-Seed Shell Using KOH for CO2 Adsorption. Processes 7 (11).

Briceño, S. et al, 2021. Diatoms decorated with gold nanoparticles by In-situ and Ex-situ methods for in vitro gentamicin release. Mater. Sci. Eng., C 123, 112018.

Cardoso-Vera, J.D. et al, 2021. A review of antiepileptic drugs: Part 1 occurrence, fate in aquatic environments and removal during different treatment technologies. Sci. Total Environ. 768, 145487.

Chávez, V. et al, 2020. Massive influx of pelagic Sargassum spp. on the coasts of the Mexican Caribbean 2014–2020: challenges and opportunities. Water 12 (10), 2908.

Cleuvers, M., 2004. Mixture toxicity of the anti-inflammatory drugs diclofenac, ibuprofen, naproxen, and acetylsalicylic acid. Ecotoxicol. Environ. Saf. 59 (3), 309–315.

Coimbra, R.N. et al, 2018. Utilization of non-living microalgae biomass from two different strains for the adsorptive removal of diclofenac from water. Water 10 (10), 1401.

Conde-Rivera, L.R. et al, 2021. TiO2 supported on activated carbon from tire waste for ibuprofen removal. Mater. Lett. 291, 129590.

Costa, R.L.T. et al, 2021. Removal of non-steroidal anti-inflammatory drugs (NSAIDs) from water with activated carbons synthetized from waste murumuru (Astrocaryum murumuru Mart.): Characterization and adsorption studies. J. Mol. Liq. 343, 116980.

Cui, X. et al, 2017. Dual functional N-and S-co-doped carbon dots as the sensor for temperature and Fe3 + ions. Sens. Actuators, B 242, 1272–1280.

Dalal, S.R. et al, 2021a. Characterization of alginate extracted from Sargassum latifolium and its use in Chlorella vulgaris growth promotion and riboflavin drug delivery. Sci. Rep. 11 (1), 1–17.

Dalecka, B. et al, 2021. Removal of pharmaceutical compounds from municipal wastewater by bioaugmentation with fungi: An emerging strategy using fluidized bed pelleted bioreactor. Environmental Advances 5, 100086.

Damarla, K. et al, 2020. DES-N-doped oxygenated carbon dot colloidal solutions for light harvesting and bio-imaging applications. Materials Advances 1 (9), 3476–3482.

de Oliveira, G.G.G. et al, 2017. Compatibility study of paracetamol, chlorpheniramine maleate and phenylephrine hydrochloride in physical mixtures. Saudi Pharmaceutical Journal 25 (1), 99–103.

de Wilt, A. et al, 2016. Micropollutant removal in an algal treatment system fed with source separated wastewater streams. J. Hazard. Mater. 304, 84–92.

Elshikh, M.S. et al, 2022. Diclofenac removal from the wastewater using activated sludge and analysis of multidrug resistant bacteria from the sludge. Environ. Res. 208, 112723.

Escapa, C. et al, 2017. Paracetamol and salicylic acid removal from contaminated water by microalgae. J. Environ. Manage. 203, 799–806.

Fernando, K.A.S. et al, 2015. Carbon quantum dots and applications in photocatalytic energy conversion. ACS Appl. Mater. Interfaces 7 (16), 8363–8376.

Fokunang, C. et al, 2018. Overview of non-steroidal anti-inflammatory drugs (nsaids) in resource limited countries. Moj Toxicol 4 (1), 5–13.

Frisch, M., et al. (2016). "Gaussian 16 Revision C. 01, 2016." Gaussian Inc. Wallingford CT 1.

Gu, Y. et al, 2019. Adsorption and photocatalytic removal of Ibuprofen by activated carbon impregnated with TiO2 by UV–Vis monitoring. Chemosphere 217, 724–731.

Helmiyati and M. Aprilliza,, 2017. Characterization and properties of sodium alginate from brown algae used as an ecofriendly super-absorbent. IOP Conference Series: Materials Science and Engineering 188, 012019.

Hifney, A.F. et al, 2021. Biosorption of ketoprofen and diclofenac by living cells of the green microalgae Chlorella sp. Environ. Sci. Pollut. Res. 28 (48), 69242–69252.

Higareda, A. et al, 2019. Synthesis of Au@Pt Core—Shell Nanoparticles as Efficient Electrocatalyst for Methanol Electro-Oxidation. Nanomaterials 9 (11).

Huang, L. et al, 2021. Adsorptive removal of pharmaceuticals from water using metal-organic frameworks: a review. J. Environ. Manage. 277, 111389.

Jellali, S. et al, 2011. Biosorption characteristics of ammonium from aqueous solutions onto Posidonia oceanica (L.) fibers. Desalination 270 (1), 40–49.

Jurado, A. et al, 2021. Urban Groundwater Contamination by Non-Steroidal Anti-Inflammatory Drugs. Water 13 (5).

Kavitha, N. et al, 2019. Formulation of alginate based hydrogel from brown seaweed, Turbinaria conoides for biomedical applications. Heliyon 5 (12), e02916.

Khadir, A. et al, 2020. Preparation of a nano bio-composite based on cellulosic biomass and conducting polymeric nanoparticles for ibuprofen removal: kinetics, isotherms, and energy site distribution. Int J Biol Macromol 162, 663–677.

Khanmohammadi, M. et al, 2012. Simultaneous determination of paracetamol and codeine phosphate in tablets by TGA and chemometrics. Thermochim Acta 530, 128–132.

Kitajima, M. et al, 2020. SARS-CoV-2 in wastewater: State of the knowledge and research needs. Sci. Total Environ. 739, 139076.

Krstić, V., 2021. Chapter 14 - Role of zeolite adsorbent in water treatment. In: Bhanvase, B., Sonawane, S., Pawade, V., Pandit, A. (Eds.), Handbook of Nanomaterials for Wastewater Treatment. Elsevier, pp. 417–481.

Lapworth, D.J. et al, 2012. Emerging organic contaminants in groundwater: A review of sources, fate and occurrence. Environ. Pollut. 163, 287–303.

Li, C. et al, 2022. Degradation kinetics and removal efficiencies of pharmaceuticals by photocatalytic ceramic membranes using ultraviolet light-emitting diodes. Chem. Eng. J. 427, 130828.

Liu, Y. et al, 2022. Enhanced removal of diclofenac via coupling Pd catalytic and microbial processes in a H2-based membrane biofilm reactor: Performance, mechanism and biofilm microbial ecology. Chemosphere 135597.

López-Miranda, J.L. et al, 2020. Evaluation of a dynamic bioremediation system for the removal of metal ions and toxic dyes using Sargassum Spp. Journal of Marine Science and Engineering 8 (11), 899.

Lung, I. et al, 2021. Evaluation of CNT-COOH/MnO2/Fe3O4 nanocomposite for ibuprofen and paracetamol removal from aqueous solutions. J. Hazard. Mater. 403, 123528.

Luo, Y. et al, 2014. A review on the occurrence of micropollutants in the aquatic environment and their fate and removal during wastewater treatment. Sci. Total Environ. 473–474, 619–641.

Madikizela, L.M., Ncube, S., 2021. Occurrence and ecotoxicological risk assessment of non-steroidal anti-inflammatory drugs in South African aquatic environment: What is known and the missing information? Chemosphere 280, 130688.

Mahmoud, M.E. et al, 2021. Effective removal of levofloxacin drug and Cr(VI) from water by a composed nanobiosorbent of vanadium pentoxide@chitosan@MOFs. Int J Biol Macromol 188, 879–891.

Marchlewicz, A. et al, 2017. Toxicity and biodegradation of ibuprofen by Bacillus thuringiensis B1(2015b). Environ. Sci. Pollut. Res. 24 (8), 7572–7584.

Miranda, J.L.L. et al, 2021. "Commercial Potential of Pelagic Sargassum spp. In Mexico." Frontiers In MarIne Science.

Mir-Tutusaus, J.A. et al, 2016. Continuous treatment of non-sterile hospital wastewater by Trametes versicolor: how to increase fungal viability by means of operational strategies and pretreatments. J. Hazard. Mater. 318, 561–570.

Mkaddem, H. et al, 2022. Anti-inflammatory drug diclofenac removal by a synthesized MgAl layered double hydroxide. J. Mol. Liq. 359, 119207.

Moradi, O. et al, 2022. Removal of pharmaceuticals (diclofenac and amoxicillin) by maltodextrin/reduced graphene and maltodextrin/reduced graphene/copper oxide nanocomposites. Chemosphere 299, 134435.

Nava-Andrade, K. et al, 2021. Layered double hydroxides and related hybrid materials for removal of pharmaceutical pollutants from water. J. Environ. Manage. 288, 112399.

Negarestani, M. et al, 2020. Simultaneous removal of acetaminophen and ibuprofen from underground water by an electrocoagulation unit: Operational parameters and kinetics. Groundwater Sustainable Dev. 11, 100474.

Neha, R. et al, 2021. Nano-adsorbents an effective candidate for removal of toxic pharmaceutical compounds from aqueous environment: A critical review on emerging trends. Chemosphere 272, 129852.

Nieto-Juárez, J.I. et al, 2021. Pharmaceuticals and environmental risk assessment in municipal wastewater treatment plants and rivers from Peru. Environ. Int. 155, 106674.

Omotola, E.O., Olatunji, O.S., 2020. Quantification of selected pharmaceutical compounds in water using liquid chromatography-electrospray ionisation mass spectrometry (LC-ESI-MS). Heliyon 6 (12), e05787.

Osafo, N. et al, 2017. Mechanism of action of nonsteroidal anti-inflammatory drugs. Nonsteroidal anti-inflammatory drugs, 1–5.

Paraguay-Delgado, F. et al, 2020. Pelagic Sargassum spp. capture CO2 and produce calcite. Environ. Sci. Pollut. Res. 27 (20), 25794–25800.

Parolini, M., 2020. Toxicity of the Non-Steroidal Anti-Inflammatory Drugs (NSAIDs) acetylsalicylic acid, paracetamol, diclofenac, ibuprofen and naproxen towards freshwater invertebrates: A review. Sci. Total Environ. 740, 140043.

Parus, A. et al, 2020. Investigation of acetaminophen adsorption with a biosorbent as a purification method of aqueous solution. Chem. Ecol. 36 (7), 705–725.

Pholosi, A. et al, 2020. Intraparticle diffusion of Cr(VI) through biomass and magnetite coated biomass: A comparative kinetic and diffusion study. S. Afr. J. Chem. Eng. 32, 39–55.

Pomati, F. et al, 2004. Effects of erythromycin, tetracycline and ibuprofen on the growth of Synechocystis sp. and Lemna minor. Aquat. Toxicol. 67 (4), 387–396.

Praveenkumarreddy, Y. et al, 2021. Assessment of non-steroidal anti-inflammatory drugs from selected wastewater treatment plants of Southwestern India. Emerging Contaminants 7, 43–51.

Puga, A. et al, 2021. Electro-reversible adsorption as a versatile tool for the removal of diclofenac from wastewater. Chemosphere 280, 130778.

Reinstadler, V. et al, 2021. Monitoring drug consumption in Innsbruck during coronavirus disease 2019 (COVID-19) lockdown by wastewater analysis. Sci. Total Environ. 757, 144006.

Riahi, K., et al. (2017). "A kinetic modeling study of phosphate adsorption onto Phoenix dactylifera L. date palm fibers in batch mode." Journal of Saudi Chemical Society 21: S143-S152.

Robledo, D. et al, 2021. Challenges and opportunities in relation to Sargassum events along the coast of the Caribbean Sea. Front. Mar. Sci. 8, 1000.

Rupani, P.F. et al, 2020. Coronavirus pandemic (COVID-19) and its natural environmental impacts. Int. J. Environ. Sci. Technol. 17 (11), 4655–4666.

Sahoo, T. R. and B. Prelot (2020). Chapter 7 - Adsorption processes for the removal of contaminants from wastewater: the perspective role of nanomaterials and nanotechnology. Nanomaterials for the Detection and Removal of Wastewater Pollutants. B. Bonelli, F. S. Freyria, I. Rossetti and R. Sethi, Elsevier: 161-222.

Sajid, M. et al, 2022. Adsorption characteristics of paracetamol removal onto activated carbon prepared from Cannabis sativum Hemp. Alexandria Engineering Journal 61 (9), 7203–7212.

Samir, E.A. et al, 2016. Hexavalent Chromium Uptake from Aqueous Solutions using Raw Biomass of the Invasive Brown Seaweed Sargassum muticum from the Moroccan Shorelines: Kinetics and Isotherms. European Scientific Journal 12, 243–262.

Santaeufemia, S. et al, 2018. Biosorption of ibuprofen from aqueous solution using living and dead biomass of the microalga Phaeodactylum tricornutum. J. Appl. Phycol. 30 (1), 471–482.

Santos, L.H. et al, 2010. Ecotoxicological aspects related to the presence of pharmaceuticals in the aquatic environment. J. Hazard. Mater. 175 (1–3), 45–95.

Shakil, M.H. et al, 2020. COVID-19 and the environment: A critical review and research agenda. Sci. Total Environ. 745, 141022.

Shang, J. et al, 2021. A novel graphene oxide-dicationic ionic liquid composite for Cr(VI) adsorption from aqueous solutions. J. Hazard. Mater. 416, 125706.

Sinurat, E. et al, 2016. Immunostimulatory activity of brown seaweed-derived fucoidans at different molecular weights and purity levels towards white spot syndrome virus (WSSV) in shrimp Litopenaeus vannamei. Journal of Applied Pharmaceutical Science 6 (10), 82–91.

Sui, Q. et al, 2015. Occurrence, sources and fate of pharmaceuticals and personal care products in the groundwater: A review. Emerging Contaminants 1 (1), 14–24.

Terauchi, M. et al, 2016. Distribution of alginate and cellulose and regulatory role of calcium in the cell wall of the brown alga Ectocarpus siliculosus (Ectocarpales, Phaeophyceae). Planta 244 (2), 361–377.

Thalla, A.K., Vannarath, A.S., 2020. Occurrence and environmental risks of nonsteroidal anti-inflammatory drugs in urban wastewater in the southwest monsoon region of India. Environ. Monit. Assess. 192 (3), 193.

Usman, M. et al, 2020. Environmental side effects of the injudicious use of antimicrobials in the era of COVID-19. Sci. Total Environ. 745, 141053.

Vaiano, V. et al, 2018. UV-LEDs floating-bed photoreactor for the removal of caffeine and paracetamol using ZnO supported on polystyrene pellets. Chem. Eng. J. 350, 703–713.

Vázquez-Delfín, E. et al, 2021. Species composition and chemical characterization of Sargassum influx at six different locations along the Mexican Caribbean coast. Sci. Total Environ. 795, 148852.

Wu, F.-C. et al, 2009a. Characteristics of Elovich equation used for the analysis of adsorption kinetics in dye-chitosan systems. Chem. Eng. J. 150 (2), 366–373.

Wu, F.-C. et al, 2009b. Initial behavior of intraparticle diffusion model used in the description of adsorption kinetics. Chem. Eng. J. 153 (1), 1–8.

Wu, G. et al, 2021. Facile fabrication of rape straw biomass fiber/β-CD/Fe3O4 as adsorbent for effective removal of ibuprofen. Ind. Crops Prod. 173, 114150.

Xiong, P. et al, 2021. Adsorption removal of ibuprofen and naproxen from aqueous solution with Cu-doped Mil-101 (Fe). Sci. Total Environ. 797, 149179.

Yuan, Y. et al, 2017. Doxorubicin-loaded environmentally friendly carbon dots as a novel drug delivery system for nucleus targeted cancer therapy. Colloids Surf., B 159, 349–359.

Yunus, A.P. et al, 2020. COVID-19 and surface water quality: Improved lake water quality during the lockdown. Sci. Total Environ. 731, 139012.

Zhang, K. et al, 2020. Ibuprofen and diclofenac impair the cardiovascular development of zebrafish (Danio rerio) at low concentrations. Environ. Pollut. 258, 113613.

Zhang, J. et al, 2021. Monitoring water-immiscible organic liquid contaminations on water via stable sensing silicone rubber composites. Mater. Lett. 305, 130827.